HYDROLOGICAL PROCESSES
Hydrol. Process. (2008)
Published online in Wiley InterScience
(www.interscience.wiley.com) DOI: 10.1002/hyp.7054

Evaluation of three evaporation estimation methods in a Canadian prairie landscape

Robert N. Armstrong,[1]* John W. Pomeroy[1] and Lawrence W. Martz[1,2]

[1] *Centre for Hydrology, Department of Geography, University of Saskatchewan, 117 Science Place, Saskatoon, Saskatchewan, S7N 5C8, Canada*
[2] *Dean of Graduate Studies and Research, University of Saskatchewan, 105 Administration Place, Saskatoon, Saskatchewan, S7N 5A2, Canada*

Abstract:

Three approaches to estimating actual evaporation (evaporation from water, soil, and transpiration from plants) are evaluated against eddy covariance observations taken during the summer period of 2006 over an upland mixed-grass site in the St Denis National Wildlife Area, central Saskatchewan. The Penman–Monteith (P–M) combination approach explicitly takes into consideration the influence of surface resistance and available energy in order to calculate evaporation from non-saturated surfaces. The Granger and Gray (G–D) expression is an extension of the Penman equation to the case of non-saturated surfaces using a complimentary approach that considers the relative evaporation G, or the ratio of actual to potential evaporation as an inverse function of the relative drying power of the air, D. D is a function of the humidity deficit and available energy. The Dalton-type bulk transfer (BT) approach typically applied in land surface schemes considers turbulent transfer along the humidity gradient between the surface and atmosphere as diagnosed from the land surface temperature. In this case, surface temperature was observed radiometrically rather than modelled. The models were evaluated for several temporal scales from 15 min to seasonal, and compared with measured evaporation data obtained by an eddy covariance system. Results suggest that all three approaches have 'reasonable' applicability for estimating evaporation at point-scales for periods longer than daily, but none of the methods provide consistently reliable daily or sub-daily estimates of evaporation. Copyright © 2008 John Wiley & Sons, Ltd.

KEY WORDS evaporation; eddy covariance; Penman–Monteith; complimentary evaporation; bulk transfer; canopy resistance; surface temperature; land surface scheme; prairie hydrology

Received 27 June 2007; Accepted 19 March 2008

INTRODUCTION

Spatially variable topography, vegetation and available water are inherent in natural landscapes but violate the steady-state assumptions of most evaporation models. Complex interactions within the soil-vegetation-atmosphere system present difficulties for reliably estimating evaporative fluxes from the land surface to the atmosphere. Accurate estimates of large-scale fluxes of water vapour (also heat and momentum) are needed for reliably predicting changes in regional weather patterns and potential changes in climate, and for the surface water balance. Estimates of these fluxes for atmospheric modelling purposes are typically provided via land surface schemes (Sellers *et al*., 1997). For the surface water balance, fluxes are provided from either land surface schemes or aggregate values from physically based, spatially distributed hydrological models (Pomeroy *et al*., 2007).

Estimates of water vapour fluxes to the atmosphere may also be provided by physically based, point-scale models (Stannard, 1993). Methods available for estimating point-scale evaporation (includes water losses via evaporation from soil and exposed water, and transpiration from plants) can vary widely as a result of different theoretical approaches and data requirements (Brutsaert, 1982). In general, the application and reliability of these approaches for providing estimates that are in close agreement with observed values typically depends on site-specific calibrations and/or experimental correction factors. These calibrations and corrections are often derived from a range of observed surface and atmospheric conditions over specific temporal scales. As a result, most evaporation estimation methods lack universal applicability, and many may not be suitable for use under a full range of surface and atmospheric conditions encountered in natural environments.

Reliably estimating evaporation for various modelling purposes also partly depends on whether a model provides estimates of 'actual' or 'potential' evaporation. In general, 'potential' evaporation may be defined as the amount of evaporation that would occur if there was an abundant supply of available water (Brutsaert, 1982). In contrast, estimates of 'actual' evaporation or the evaporation that actually enters the atmosphere from the earth's surface is required for modelling hydrological and atmospheric processes. A standard practice has been to estimate the actual evaporation as some fraction of the potential evaporation (Granger, 1989). In sub-humid environments such as those found across the Canadian

* Correspondence to: Robert N. Armstrong, Centre for Hydrology, Department of Geography, University of Saskatchewan, 117 Science Place, Saskatoon, Saskatchewan, S7N 5C8, Canada.
E-mail: robert.armstrong@usask.ca

prairies, potential evaporation is normally well in excess of actual evaporation. As a result, it may be difficult to apply simple linear adjustments to obtain reliable estimates of the actual evaporation.

In sub-humid to arid environments, actual evaporation is primarily governed by water supply, and potential evaporation by energy supply. A further complication arises in that the concept of potential evaporation generally lacks a clear and universally accepted definition (Granger, 1989). The relative differences between definitions depend on the specific surface and/or atmospheric conditions that are considered important for estimating the potential evaporation. Alternatively, the combination equation of Penman (1948) provides a useful approach for estimating potential evaporation from a saturated surface, while eliminating the need for estimates of surface temperature. Granger and Gray (1989) have taken advantage of this by introducing the relative evaporation or ratio of actual to potential, through a complimentary relationship which can be used to directly estimate actual evaporation from non-saturated surfaces.

For the purpose of this study, three physically based approaches for estimating 'actual' evaporation in the prairie landscape are considered: (1) a combination model; (2) a complimentary combination model; and (3) a surface temperature bulk transfer (BT) model. For the first method, the Penman–Monteith (P–M) (Monteith, 1965) model was selected. The P–M model is a combination energy balance and aerodynamic extension of the Penman (1948) equation to non-saturated surfaces that explicitly considers the control of plants on transpiration via plant stomata. The canopy resistance term introduced in the P–M method exerts a major control on plant transpiration in response to environmental factors such as soil moisture, incoming solar radiation, humidity, and air temperature (Jarvis, 1976). Stannard (1993) describes the original P–M equation (used for this article) as a big leaf model applicable to a full canopy (i.e. limited exposure of bare soil between plants).

For the second method, the Granger and Gray (1989) model was selected. The Granger and Gray (G–D) complimentary relationship evaporation model is an extension of the combination model of Penman (1948) and the complimentary approach introduced by Bouchet (1963). The basic principle of the complimentary approach is that actual evaporation declines as the land surface dries under conditions of decreasing water availability whilst potential evaporation increases. The G–D method applies the Penman equation to non-saturated surfaces by introducing the relative evaporation ratio G, which is a non-linear function of the drying power of the atmosphere which itself is a function of the humidity deficit and available energy. An attractive feature of this equation is that it does not require the factors used by the Jarvis algorithm to estimate canopy resistance. While feedback relationships between the surface and atmosphere may be apparent, and the relationship works well (Granger and Pomeroy, 1997), the physical basis of the mechanisms influencing these relationships has still not been fully described (Crago and Crowley, 2005; Lhomme and Guilioni, 2006).

For the third method, the Dalton-type BT model was selected. In 1802, Dalton showed that the rate of evaporation from a water surface is directly proportional to the differences between the saturation vapour pressures at the surface temperature of the water and the dew point of the air (Penman, 1947). In the BT model applied here, surface temperature is used to estimate the saturated specific humidity at the surface of the canopy. The implicit assumption in this method is that leaf sub-stomatal cavities are saturated at the temperature of the leaf surface (Verseghy *et al*., 1993). The humidity gradient can then be determined between the surface, and that measured at some reference height above the surface, from the air temperature and relative humidity (RH). The flux of water vapour along this gradient also takes into consideration the aerodynamic resistance of the canopy via turbulent transfer, the logarithmic wind profile, and the canopy resistance.

The BT approach is widely used for estimating surface fluxes and is commonly applied in land surface parameterization schemes (Mahrt, 1996; Sellers *et al*., 1997). This may be attributed in part because the method, (1) can be relatively simple to apply; (2) is driven by surface temperature which is commonly diagnosed by iterative solutions to the surface energy balance in land surface schemes; and (3) provides a direct estimate of the flux gradient between the surface and atmosphere. The BT method may also be applied to both land surfaces and open water surfaces, and has the potential for directly integrating remotely sensed surface temperature data obtained via field measurements, or derived from airborne or satellite imagery.

The P–M, G–D, and BT models evaluated in this prairie landscape study were chosen specifically because they, (1) are physical-based; (2) provide estimates of 'actual' evaporation which is typically needed for modelling hydrological and atmospheric processes; and (3) represent contrasting theoretical approaches. Also, the G–D complimentary relationship was developed from field observations that included the Canadian prairie and boreal forest regions (i.e. relevant local applicability). The objective of this article is to evaluate point-scale 'actual' evaporation estimates provided by the three models against observations obtained using the eddy covariance method in a prairie environment. The soil moisture conditions within the upper 30 cm profile range from well watered to relatively dry over the course of the observation period; approximately 45–20% volumetric soil moisture content. Modelled evaporation estimates during the growing season period (extending from late May to early September) of 2006 are derived from 15-min averages, and compared to the observed values for several optimal data periods including 15 min, daily, multi-day and 69 days of observations.

DOI: 10.1002/hyp

FIELD SITE

The field site was located in the St Denis National Wildlife Area (SDNWA) approximately 40 km east (52°12′N 106°55′W) of Saskatoon, Saskatchewan, Canada (Figure 1). Elevations in the area range from approximately 540 to 565 m. The landscape consists of moderately rolling knob and kettle moraine, which is typical of much of the prairie region of western Canada. SDNWA is located in the dark brown Chernozem soil region of the prairies where soils are generally fine textured (silty loams) with parent materials typically consisting of clay-rich glacial tills (van der Kamp *et al*., 2003).

A reference evaporation study site located on an upland plateau is characterized by gently rolling hummocky hill terrain (slopes <2%) which gives way to steeper downslope rolling terrain (slopes of 10–15%). In 2004, the reference area was seeded to a mix of cool-season C_3 grasses (Yates *et al*., 2006). In 2006, the most established species included several wheat grasses (*Agropyron elongatum, Agropyron intermedium, and Agropyron trachycaulum*) and two forage crops; alfalfa (*Medicago sativa*) and sainfoin (*Onobrychis viciifolia*).

METHODS

Measuring evaporation: eddy covariance method

Observations of evaporation were obtained using the eddy covariance method. This is the most direct method for measuring turbulent fluxes of water vapour, heat, and momentum (Brutsaert, 1982). Figure 2 shows the tripod mast eddy covariance system deployed at St Denis in the spring and summer of 2006. Turbulent fluxes of wind in the horizontal and vertical directions were measured using a three-dimensional sonic anemometer (Campbell Scientific CSAT3). Fluctuations of atmospheric water vapour were measured using an ultraviolet krypton hygrometer (Campbell Scientific KH20). The fluxes of water vapour and heat were corrected using a planar-fit axis rotation and correction algorithm (Wilczak *et al*., 2001).

The tripod mast was placed at the upland reference site for the entire study period extending from 19 May to 11 Sept 2006. Modelled estimates are evaluated against observations collected at the mast. A fetch to height ratio of 1 : 100 was used such that the eddy covariance instruments were placed at a height of between 1 and 1·5 m above the canopy throughout the measurement period to remain within the boundary layer of the reference site. The leading edge of the reference grass site (bordered by cultivated land) is located approximately 150 m upwind.

Continuous micrometeorological measurements collected at the reference site were used to parameterize the evaporation models for evaluation purposes. Specific data required for this are: net radiation for the energy balance requirements of the Penman-type models (Kipp and Zonen CNR1 net radiometer); ground heat flux

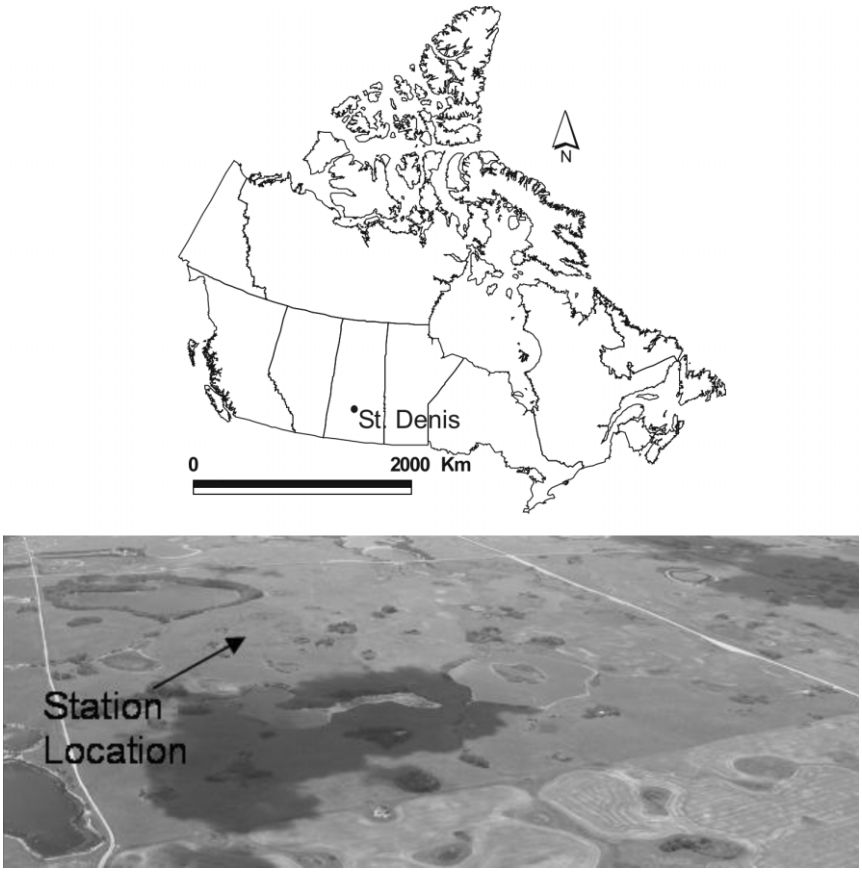

Figure 1. Geographical location of eddy covariance station and aerial photo of St Denis National Wildlife Area (July, 2006)

DOI: 10.1002/hyp

Figure 2. Eddy covariance system and land surface vegetation at St Denis National Wildlife Area

for calculating the available energy term (Radiation and Energy Balance (REBS) soil heat flux plate), wind speed (CSAT3), temperature and humidity (Campbell Scientific Vaisala HMP45C series probe), soil moisture data collected continuously for the upper 30 cm of the soil profile (Campbell Scientific CS616 water content reflectometer) for estimating the canopy resistance, and surface temperature (Exergen infrared thermocouple (IRTC) temperature sensor).

ESTIMATING EVAPORATION

Penman–Monteith (P–M) method

The general form of the Penman–Monteith (P–M) equation (Monteith, 1965) is an extension of the Penman combination energy balance and water vapour transport equation to non-saturated surfaces,

$$E = \frac{\Delta \dfrac{(Q_n - Q_g)}{\lambda} + \left(\rho C_p \dfrac{(e_a^* - e_a)}{r_a}\right)}{\Delta + \gamma\left(1 + \dfrac{r_c}{r_a}\right)} \tag{1}$$

where Δ is the slope of the saturation vapour pressure curve calculated as a function of temperature, T,

$$\Delta = \frac{4098\left[0{\cdot}6108\exp\left(\dfrac{17{\cdot}27T}{T+237{\cdot}3}\right)\right]}{(T+237{\cdot}3)^2}. \tag{2}$$

Q_n and Q_g are net radiation and ground heat flux (W m^{-2}) respectively, λ is the latent heat of vapourization (kJ kg^{-1}) which is slightly dependent on temperature, T (°C) which is found as $2501-2{\cdot}361(T)$, ρ is the air density (kPa), Cp is the specific heat of air (1·005 kJ kg^{-1}), e^*_a and e_a are the saturated and actual vapour pressures of the air (kPa), γ is the psychometric constant (kPa °C^{-1}), and r_a and r_c are the aerodynamic and canopy resistances (m day^{-1}). This method first introduced the control exerted by plants on the transfer of water vapour to the atmosphere via stomatal openings mainly found on the underside of leaves.

Granger and Gray (G–D) method

The method developed by Granger and Gray (1989) is based on the complimentary relationship introduced by Bouchet (1963), and also extends the Penman equation to non-saturated surfaces by introducing the relative evaporation ratio, G,

$$E = \frac{\Delta G \dfrac{(Q_n - Q_g)}{\lambda} + \gamma G E_A}{\Delta G + \gamma} \tag{3}$$

where E_A represents the drying power of the air which can be found using the Dalton-type formulation $f(u)(e^*_a - e_a)$ and $f(u)$ is a vapour transfer function found as (Pomeroy *et al*., 1997),

$$f(u) = 8{\cdot}19 + 22z_0 + (1{\cdot}16 + 8z_0)u \tag{4}$$

where $z_0 = h/7{\cdot}6$ is the aerodynamic roughness length (m), h is vegetation height (m), and u is the wind speed (m s^{-1}). The relative evaporation parameter is based on observations obtained over a variety of surfaces in the prairie, arctic, sub-alpine, and boreal forest regions of western Canada, and can be obtained by,

$$G = \frac{1}{0{\cdot}793 + 0{\cdot}2e^{4{\cdot}902D}} + 0{\cdot}006D \tag{5}$$

which is related to the relative drying power of the air obtained as a function of the humidity deficit and the available energy,

$$D = \frac{E_A}{E_A + \dfrac{(Q_n - Q_g)}{\lambda}} \tag{6}$$

Dalton-type bulk transfer (BT) method

The bulk transfer (BT) formula applied for this study is similar to that used for the vegetation component of the Canadian Land Surface Scheme (CLASS) by Verseghy *et al*. (1993). Rather than being driven by the model diagnosis of surface temperature from an iterative solution to closing the surface energy balance, the BT model applied in this study is driven by surface temperature observations. The simple parameterization used here requires

DOI: 10.1002/hyp

measurements or estimates of air density, surface temperature, vapour pressure, wind speed, vegetation height, and soil moisture used in the calculation of r_c:

$$E = \frac{\lambda\rho(q_s(T_s) - q)}{r_a + r_c} \quad (7)$$

where q_s is the saturated specific humidity (kg kg^{-1}) at the surface temperature (T_s), and q is the specific humidity of the air (kg kg^{-1}).

Aerodynamic and canopy resistances

Application of the P–M and BT equations to non-saturated surfaces requires consideration of the resistances of water vapour transfer to the atmosphere. Estimates of the aerodynamic resistance are obtained assuming a logarithmic wind profile formulation:

$$r_a = \frac{\left[\ln \frac{(z-d)}{z_0}\right]^2}{k^2 u} \quad (8)$$

where u is the wind speed at the reference height, z, $d = 0{\cdot}67\ h$, is the displacement height of the vegetation (m), and k is the von Kármán constant (0·41). Vegetation height data were collected over the summer, and a simple linear interpolation was used to produce a continuous dataset of vegetation heights over the period. The measured vegetation height ranged from 0·1–0·2 m in mid-May to 1–1·2 m in early July.

Estimates of canopy resistance were obtained using the general model proposed by Jarvis (1976) and the experimental relationships developed by Verseghy *et al.* (1993) for the multiplicative factors describing environmental stress effects on stomatal control:

$$r_c = r_{c\,min} f_1 f_2 f_3 f_4 \quad (9)$$

where $r_{c\,min}$ represents the minimum unstressed canopy resistance (s m^{-1}). The multiplicative factors describe stomatal control as a representative value of 1 under what may be considered optimal conditions for plant growth, and a value >1 under stressed conditions. f_1 increases under conditions when light is limiting, and is a function of the incoming solar radiation, $K\downarrow$ (W m^{-2}) required for photosynthesis,

$$f_1(K\downarrow) = \max(1{\cdot}0, (500/\mathrm{K}\downarrow - 1{\cdot}5)). \quad (10)$$

f_2 is a function of the vapour pressure, e, deficit (mb) required to maintain water and nutrient uptake to the plant, which increases as the plant's ability to transmit water from the soil rooting zone is exceeded,

$$f_2(\Delta e) = \max(1{\cdot}0, (\Delta e/5{\cdot}0)). \quad (11)$$

f_3 is a function of soil moisture supply, specifically the soil moisture tension, ψ (m) which increases with decreasing soil moisture,

$$f_3(\psi) = \max(1{\cdot}0, \psi/40{\cdot}0) \quad (12)$$

where ψ is derived for the current study using the Campbell power law function for specific soil texture classes based on the air entry tension ψ_{ae}, porosity ϕ, a pore size distribution index b, and soil moisture θ (Campbell, 1974),

$$\psi = \psi_{ae}\left(\frac{\phi}{\theta}\right)^b. \quad (13)$$

f_4 is a function of temperature with an operating range between 0 and 40 °C

$$f_4(T) = 1{\cdot}0 \text{ if } T < 40\,^\circ\mathrm{C} \text{ and } > 0\,^\circ\mathrm{C} \quad (14)$$

OR

$$\text{if } T > 40\,^\circ\mathrm{C} \text{ or } < 0\,^\circ\mathrm{C} \text{ then } f_4(T) = 5000/r_{c\,min}$$

and indexes the range of temperatures at which transpiration may be considered to occur. The range of operating temperatures indicated above were not a factor in the current analysis since the observed daytime air temperature rarely fell below 5 °C and was seldom above 30 °C during the observation period.

ISSUES TO CONSIDER FOR A COMPARATIVE ANALYSIS

To reduce some of the uncertainty in measured evaporation using the eddy covariance method (due to missing or uncertain data values) only the observations obtained during optimal data periods were considered for evaluating the model estimates. Optimal data periods ranged from 2 days to 2 weeks in duration, in which the CSAT and krypton hygrometer were working well and for which complete field measurements were available for driving the evaporation models. During wet periods, the signal of both the CSAT and hygrometer were interrupted by water droplets that collected on the instruments. Therefore, results reported here are for periods when the instruments were dry and operational; in total, 69 days of reliable observations were collected over the period from 19 May to 11 Sept 2006.

It should be noted here that the evaporation models evaluated are driven by field observations and applied independently of a hydrological continuity approach. That is, no explicit modelling of the mass balance of soil moisture is considered to limit evaporation. The models were simply allowed to run under the measured atmospheric conditions and observations of surface temperature and soil moisture. As a result, the only calibration required is that of $r_{c\,min}$ for calculating the canopy resistance for the P–M and BT models. An advantage of the G–D model is that it does not require any calibration.

A fitted value of 62 s m^{-1} was determined for $r_{c\,min}$ to represent the unstressed conditions for the grassed surface. This is in the general range reported for grasses and crops 25–100 s m^{-1} (Verseghy *et al.*, 1993). A typical value for a lush, dense grass canopy may be

DOI: 10.1002/hyp

in the order of 50 s m^{-1}, but may be higher in the case of the less dense canopies typically found in prairie regions. At the St Denis site, a negligible amount of bare soil was visible under the plant canopy near the plant stems. As such, the site did not warrant explicitly dividing evaporation between the soil and plants using a complex two-source-model approach (i.e. resistance network) such as that of Shuttleworth and Wallace (1985).

For periods less than daily, the application of Penman-type models (P–M and G–D) and the canopy resistance term becomes somewhat problematic. This is because of the negative net supply of energy ($-Q_n$) occurring during the night. Point-scale evaporation models based on the energy balance approach are only applicable under conditions when Q_n is positive. As is often the case, the net supply of energy to the land surface during the night is negative due to the relatively large amount of long-wave radiation emitted from the surface to the atmosphere. Likewise, transpiration, which occurs during photosynthesis in C_3 carbon fixing plants (e.g. cool-season grasses) is generally restricted to daylight periods when Q_n is positive.

As a result, the G–D method was applied only to those periods where Q_n was positive and evaporation was set to zero when Q_n was negative. For the P–M and BT methods, the canopy resistance term r_c was set to 5000 s m^{-1} during periods when Q_n was negative, which typically occurred between the hours of 7 : 30 pm and 6 : 00 am at St Denis over the study period. Therefore, any occurrences of evaporation or condensation during this time period were negligible, effectively limiting all three models to be operational during daylight only.

Finally, consideration was given to stability corrections for the sub-daily periods. Typically, corrections for stability would be applied to the vapour transfer function (in the case of a Penman-type model) or the logarithmic wind profile of the aerodynamic resistance term. However, for the purpose of the present comparisons, neutral stability is assumed and no corrections for stable or unstable conditions were made. Most evaporation models have been developed under the implicit assumption of neutral stability. Corrections for stability are also typically ignored in hydrological models when point-scale evaporation equations are applied. Further, given the relatively strong surface winds observed during the daytime at St Denis, which is typical of prairie environments, the assumption of neutral stability is not considered problematic.

RESULTS AND DISCUSSION

Climate conditions during 2006 observation period at St Denis

The St Denis research site is located approximately 40 km east of the city of Saskatoon and 40 km west of the town of Humboldt, Saskatchewan, Canada. Environment Canada 1971–2000 long-term climate normals for Saskatoon and Humboldt are shown in Figure 3. On the basis of the climate normals, the central region of Saskatchewan can be classified as a sub-humid environment. Mean annual temperatures for Saskatoon and Humboldt are 2·2 and 1·5 °C, respectively. Total annual precipitation for Saskatoon is approximately 350 mm and is slightly higher for Humboldt at approximately 390 mm. For the period extending from May to September, Saskatoon has a mean temperature of 14·8 °C and Humboldt is slightly lower at 14·1 °C. At both locations, the majority of this precipitation is received during May to September (as rainfall); approximately 240 mm at Saskatoon and 275 mm at Humboldt.

A comparison of the climate normals and the 2006 climate conditions at St Denis from 19 May to 11 Sept are provided in Table I. For the current discussion, only the complete months of June to August will be examined. The mean temperature for these months at St Denis during 2006 was 18·1 °C, which is 1–2 °C higher than the normals for Saskatoon (17·1 °C) and Humboldt (16·3 °C). The largest difference in mean monthly temperatures was observed for July, approximately 2·0 °C greater compared to Saskatoon and Humboldt.

From June to August, 176 mm of precipitation was recorded at St Denis, which is between the normals for Saskatoon (160 mm) and Humboldt (195 mm). It is important to note that 95·6 mm of the total rainfall recorded at St Denis occurred during 9 non-consecutive

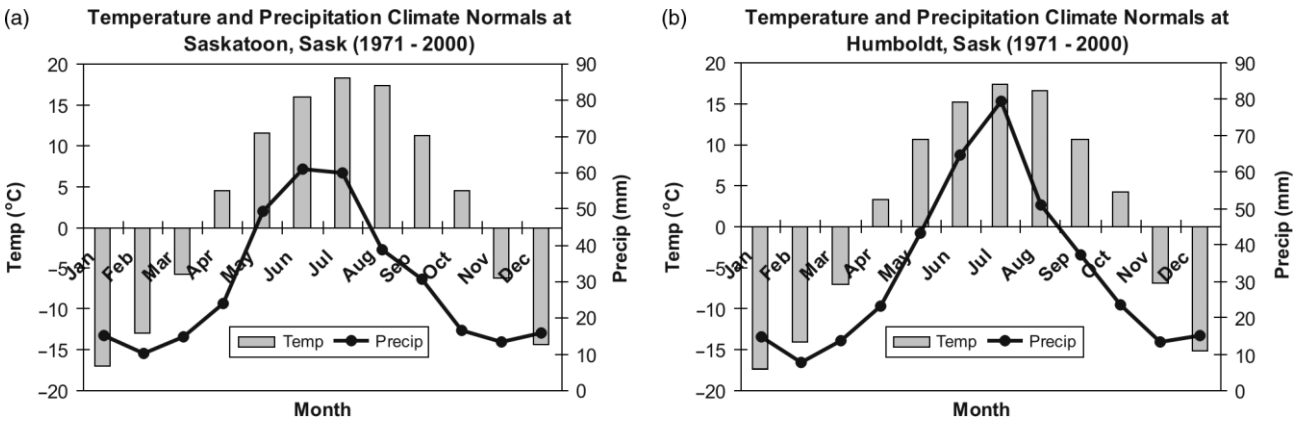

Figure 3. Climate normals for Saskatoon and Humboldt, Saskatchewan, Canada, from 1971 to 2000 (Meteorological Service of Canada)

DOI: 10.1002/hyp

Table I. 1971–2000 monthly climate normals vs observed temperature and precipitation at St Denis, Saskatchewan, from 19 May to 11 Sept 2006. Values of temperature are reported in°C, and precipitation in mm

Location	Variable	May	June	July	Aug	Sept
Saskatoon (climate normals)	Temperature	11·5	16	18·2	17·3	11·2
	Precipitation	49·4	61·1	60·1	38·8	30·1
Humboldt (climate normals)	Temperature	10·6	15·2	17·4	16·5	10·7
	Precipitation	43·4	64·8	79·3	51	37·3
St Denis (19 May -11 Sept)	Temperature	12·9	16·6	19·9	17·8	12·7
	Precipitation	14·2	96·3	23·6	56·2	0·0

days over a 12-day period in early to mid-June; approximately 30 mm higher than normal for the month. In contrast, 24 mm of rainfall was recorded in July which is only one-third the rainfall normally received at Saskatoon and Humboldt. In August, 56·2 mm of rain was recorded at St Denis, which is close to the normal rainfall for Humboldt (51 mm) and is higher than the normal rainfall for Saskatoon (38·8 mm).

Observed evaporation

The cumulative observed evaporation over 69 days of optimal data observations was 161·3 mm (2·3 mm day^{-1}). Figure 4 shows a time series of measured daily averages of evaporation, net radiation, air temperature, surface temperature, wind speed, soil moisture, RH, and estimated evaporation for the three models considered. Daily observed evaporation ranged from approximately 0·8 to 4·4 mm, peaked in late June/early July and then decreased over the course of measurements. The highest rates of evaporation typically occurred after precipitation events, primarily early in the season, and peaked during the summer blooming period. Following the peak evaporation period, there was a large decline in evaporation over the course of the season, which coincides with a trend of declining soil moisture.

In general, other climate and surface variables that drive evaporation do not show similar trends. There appeared to be no appreciable decline in net radiation until the beginning of August, nor did there appear to be a noticeable decrease in air temperature over the same period. The daily surface temperature was lower during the peak evaporation period and higher in July under conditions of declining soil moisture. As would be expected, the daily surface temperature tended to be lower immediately following wetting periods due to the increase in near-surface water availability and increase in evaporation. The surface temperature remained suppressed during the peak evaporation period, which occurred during late June. The surface temperature was also lower later in the season largely as a result of a seasonal reduction in solar radiation. Surface temperature tended to increase during drying periods, as near-surface water availability and evaporation declined, and was generally higher immediately following the peak evaporation period.

Cumulative evaporation for 69 days of observations

For comparative purposes, $r_{c\,min}$ for both the P–M and BT methods should have a common meaning. In other words, $r_{c\,min}$ should be equal in value for both models and not biased due to differences in the theoretical approaches. For this study it was found that a fitted value of 62 s m^{-1} for $r_{c\,min}$ resulted in reasonably comparable evaporation estimates for both the P–M and BT methods for the entire 69 days of optimal data observations. A comparison of cumulative observed and modelled evaporation for all 69 days is provided in Table II. Overall, the P–M, G–D, and BT model estimates were generally within 5% of the observed values. All three methods slightly underestimated the observed total evaporation. The P–M method provided the closest agreement, but underestimated the observed evaporation by 5 mm. The G–D and BT methods also underestimated the observed value by approximately 7·5 and 8·5 mm, respectively.

Multi-day evaporation estimates

A comparison of model estimates with observed values for each of the optimal data periods ranging from 2 days to 2 weeks in duration is shown in Table III. Evaporation estimates are given as cumulative totals for each optimal period. For several optimal periods, modelled evaporation estimates agree reasonably well with the observed values. No single model was shown to consistently provide the best agreement to the observed values of evaporation.

Overall, the G–D method provided the best agreement for 4 out of 10 optimal periods. These optimal periods were comprised of two 2-day periods, one 3-day period, and one 5-day period. Both the P–M and BT methods performed better than the G–D method for only 2 out of 10 optimal periods. For 2 of the optimal periods none of the models performed well, with absolute differences from the observed evaporation typically greater than 3 and 14 mm higher in the case of the BT model. Results also show that none of the models was found to consistently overestimate or underestimate evaporation compared to the observed values. In general, when

Table II. Modelled estimates vs measured evaporation (mm) accumulated over 69 days of optimal observations

Method	Cumulative (mm) over 69 days
Observed	161·3
P–M	156·2
G–D	153·6
BT	152·8

DOI: 10.1002/hyp

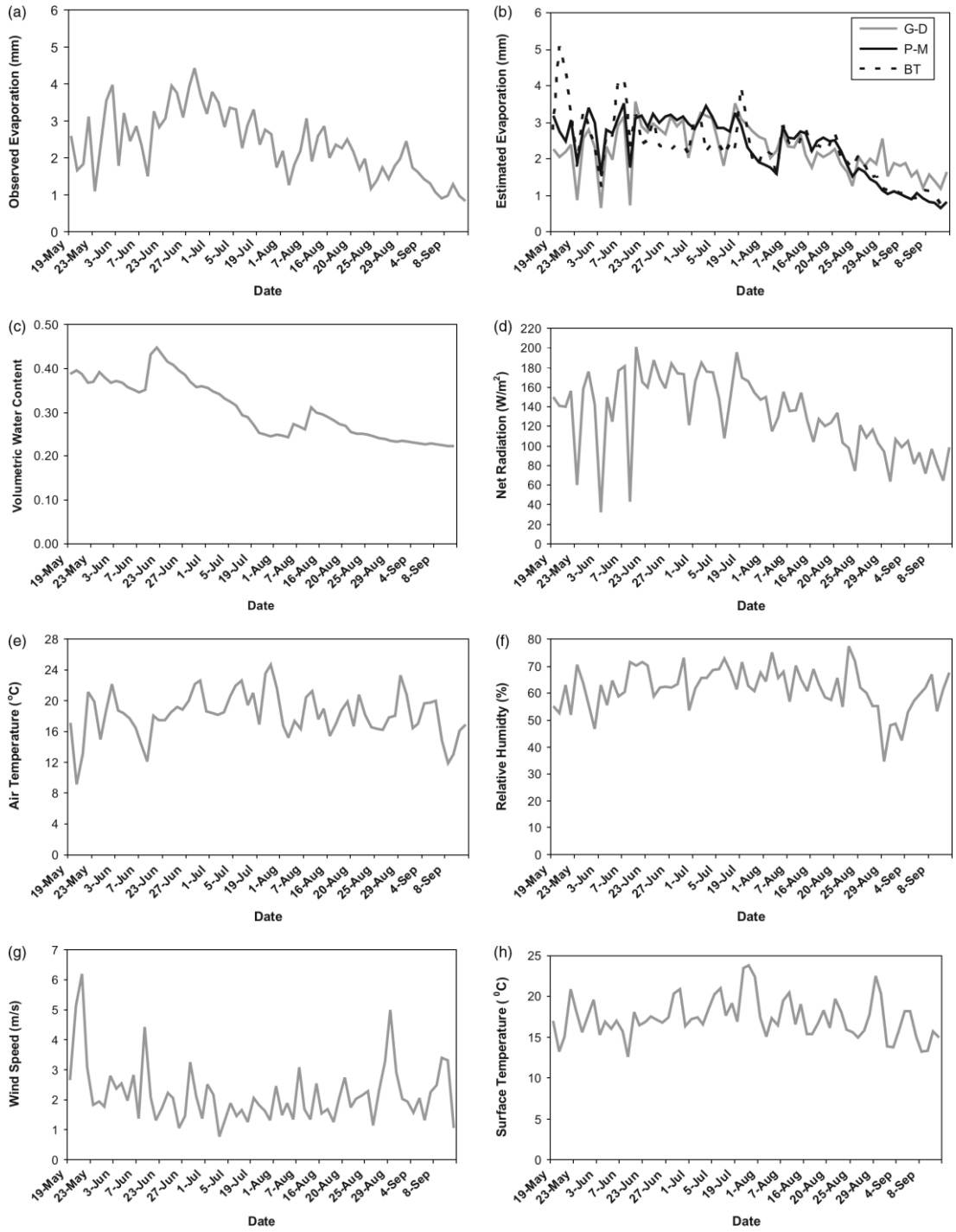

Figure 4. Measured daily averages of: (a) observed evaporation, (b) modelled evaporation estimates, (c) volumetric water content, (d) net radiation, (e) air temperature, (f) relative humidity, and (g) wind speed

compared to the G–D and P–M methods, the BT method tended to provide the poorest agreement to the observed values with the exception of the last 2 weeks of August.

In particular, the large overestimate given by the BT model during the first period (19–23 May) may be partly attributed to problems with the flux-gradient relationship derived from a small areal radiometric measurement of surface temperature. The plant and soil surface exposed for radiation transfer is not exactly the surface exposed to turbulent transfer. Another possible factor could be that of not accounting for the small leaf area early in the growing season when estimating an effective canopy resistance. For example, both the P–M and BT methods were unable to provide good estimates during the early plant growth period during 19–23 May. During this period, the P–M model overestimated the observed value by only 3 mm but the BT model was 7 mm higher. For the P–M method, the effect is likely lessened because of the increased sensible and ground heat fluxes at the surface, which reduces the energy available for evaporation. Intuitively, accounting for reduced leaf area to determine an effective higher

DOI: 10.1002/hyp

canopy resistance term would result in a further reduction of the modelled evaporation during this early growth period.

In contrast, the G–D approach, which makes no assumptions about plant leaf area or stomatal controls, provided the best agreement – to within 0·5 mm of the observed value for the same period. Such an approach has an advantage when compared to methods which rely on the parameterization of complex resistance terms. However, the P–M and BT methods provided much better estimates than the G–D method for the next period from May 31 to June 8 (Table III) when plant leaf area was no longer an issue. During this period the G–D model estimate was 5 mm less than the observed value, which suggests the relative evaporation parameter may have been too limiting.

Table III. Comparison of modelled vs observed evaporation (mm) accumulated during optimal data periods (2 days or longer)

Optimal data periods	Obs	P–M	G–D	BT
May 19–23	10·3	13·3	9·8	17·1
May 31–Jun 8	24·1	24·6	19·4	25·3
Jun 22–Jul 6	51·0	46·0	41·9	37·0
Jul 14–15	6·2	6·0	6·2	4·6
Jul 22–23	5·4	4·5	5·7	5·0
Aug 1–2	3·5	3·6	4·6	4·4
Aug 6–8	7·2	8·0	7·4	7·7
Aug 14–20	16·7	17·7	15·2	17·1
Aug 22–30	15·6	13·4	16·5	14·8
Sep 2–11	12·2	9·0	15·7	9·9
Total	152·2	146·7	142·2	142·4

Figure 5 compares the modelled estimates and observed evaporation for each of the 10 optimal periods. The one-to-one line, r^2 values and root mean squared error (RMSE) are also indicated in each graph. Overall, the P–M and G–D methods provided the best results when compared with the observed values for the optimal data periods ($r^2 = 0{\cdot}98$). The associated RMSE for each model is elevated due to the large underestimates of evaporation for the period from 22 June to 6 July; differences of 5–10 mm. Comparisons between the modelled estimates and observed values show that there tends to be a great deal of variability between estimates for any given period despite the relatively close agreement for the entire 69 days of observations.

This variability may be attributed in part to several factors: (1) the atmospheric conditions over the optimal periods tend not to be steady-state; (2) it is difficult to adequately account for energy storage at the surface; (3) the feedback mechanisms for the complimentary evaporation method (G–D) are subject to lag effects such that atmospheric changes tend to occur more slowly than do conditions at the surface; (4) the surface temperature for the BT method is measured radiometrically over a small area and does not completely represent the surface involved in turbulent exchange with the atmosphere over the variable flux footprint; (5) no assumptions have been made regarding plant phenology and health; and (6) no consideration has been given in this study for the possible effects of spatial variability in driving factors

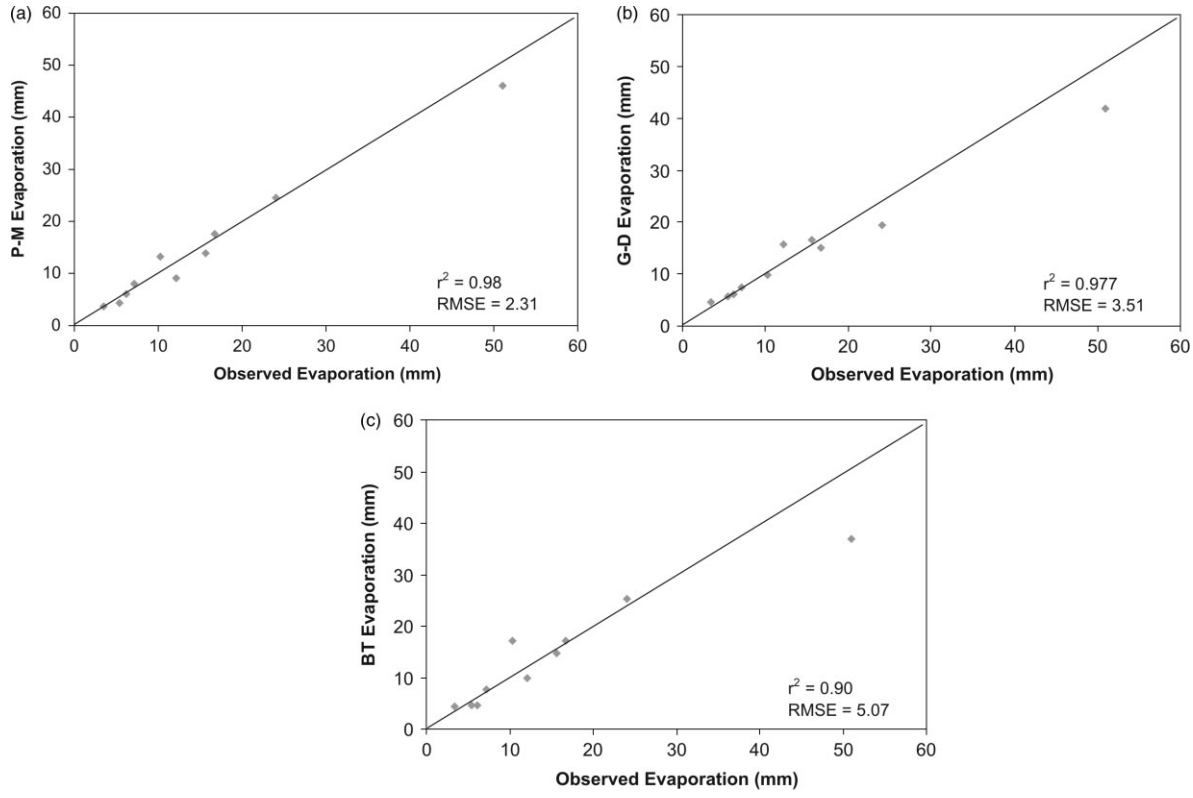

Figure 5. Optimal data period cumulative evaporation (mm), (a) P–M versus observed, (b) G–D versus observed, (c) BT versus observed. The one-to-one line is the diagonal line

DOI: 10.1002/hyp

contributing to the evaporative flux measured at the sensors.

June 22 to July 6 peak evaporation period

Modelled results for the 22 June–6 July period are of particular interest. As shown in Table III, all the models strongly underestimate the observed evaporation which totalled 51 mm during this 15-day period (3·4 mm day^{-1}). For this period, the P–M method provided the closest agreement to the observed value, underestimating evaporation by 5 mm. The G–D and BT methods underestimated the observed value by nearly 10 and 14 mm, respectively. These differences are of general interest because the observed evaporation peaked during this period of the season.

First, there are several notable reasons for the peak evaporation to occur during the 22 June–6 July time period: (1) as shown in Figure 4, water and energy availability do not appear to be limiting factors; (2) the mixed grasses, namely, wheat grasses, alfalfa, and sainfoin, were fully developed and in full bloom (blooming began in early to mid-June); (3) water use by the grasses, and most other plants in general, during the blooming period or reproductive stage of growth can be assumed to be optimal to maintain maximum photosynthesis and thus, plant activity/productivity (support for this can be found in the case of prairie grasses (Verma *et al*., 1992) and more so in the case of wheat crops Shen *et al*., 2002; Raddatz and Cummine, 2003); and (4) the leaf area of plants can reasonably be expected to be near a maximum value for an extended period prior to the onset of blooming, and through the blooming period.

Assumptions regarding plant phenology can be ignored during the peak evaporation period since there was a fully developed plant canopy. A $r_{c\,min}$ correction factor based on either a leaf area index (LAI) (leaf area per unit ground area) or fractional leaf area (fraction of ground area covered by vegetation) approach may be used to track changes in vegetation growth and reflect the relative number of stomata acting in parallel during transpiration (Verseghy *et al*., 1993; Raddatz and Cummine, 2003). It can reasonably be assumed that a correction factor would essentially be close to 1·0 during the peak evaporation period under the conditions of a full canopy and relatively dense, healthy vegetation and non-drought conditions. In the case of the G–D method, the canopy resistance of plants is not even a factor; rather, the relative evaporation parameter limits evaporation as a function of the available energy and the humidity deficit. This humidity deficit reflects the surface water availability to the atmosphere. Therefore, the possible physical basis behind the underestimations by the models and differences in the evaporation estimates compared to the observed value warrants further consideration.

One possible factor that is common to all three models is the effect of atmospheric humidity. As shown in Figure 4, the mean daily RH was fairly low; between 60 and 70% during the period of peak evaporation compared to that following the peak evaporation period. During the daytime, the RH was typically around 40% or less. In the case of the G–D method, a higher humidity deficit and the abundant supply of available energy would increase the drying power of the air, resulting in a smaller value of relative evaporation, G, thereby reducing evaporation. In the case of the P–M method, increases in the humidity deficit beyond the optimal plant operating conditions would result in an increase in the canopy resistance. The overall effects of this increase in canopy resistance, however, may be offset by the balance of available energy. In this case, there is a potential benefit of applying the P–M combination approach which could possibly explain why the P–M method provided better agreement for the peak evaporation period.

Unlike the P–M combination approach, the BT method directly considers the humidity gradient driven by measured surface temperature which itself is an implicit function of the surface energy balance. Results at the St Denis upland site show that the observed evaporation generally follows diurnal variations in surface temperature; r^2 values are typically in the order of 0·85–0·90 with some scatter. Expectedly, the observed surface temperature follows closely with diurnal variations in net available energy. This makes it difficult to use a small-scale measurement of surface temperature when the energy balance is generally considered over a larger area. Also, due to the difference in theoretical approaches of the models, the canopy resistance term appears to have a larger influence on evaporation estimates for the BT method than it does for the P–M method.

For the majority of the peak evaporation period, the daytime surface temperatures and mean daily surface temperature (typically around 16·5–17·5 °C) were generally lower than following the peak period. As shown in Figure 4, the lower surface temperatures are likely explained by the ample soil moisture in the upper 30 cm soil profile leading to increased water losses from the plants via transpiration during this phenological stage. This may point to a potential disadvantage of applying the BT method to a vegetation canopy under these conditions. That is, lower surface temperatures imply lower rates of evaporation due to the reduced surface specific humidity, all other considerations being equal. In order to improve the BT estimate compared to the observed value under the condition of lower canopy temperatures, the value of $r_{c\,min}$ would also need to be reduced to effectively increase the evaporation rate. This may help to explain why the BT method produced the largest underestimate compared to the observed value for the peak evaporation period.

As a simple test, a lower reference value of $r_{c\,min} = 50$ s m^{-1} was specified for the P–M and BT models. The resulting P–M model estimate for the 22 June–6 July period increased to 53·5 mm, which is very close to the observed value of 51 mm. The BT estimate increased to 44·8 mm compared to the previous estimate of 37 mm but was still 6·2 mm less than the observed value. However, for the entire 69 days of optimal observations,

DOI: 10.1002/hyp

the lower $r_{c\,min}$ value resulted in a large overestimate of the observed evaporation by approximately 30 mm for both the P–M and BT methods. Attempting to adjust $r_{c\,min}$ as a function of leaf area would have no beneficial effect for model performance during this period and would do little to improve the overall results for the 69 days since only the first two time periods would be affected.

These results suggest that there is a problem in using the canopy resistance term in evaporation models. That is, the value of $r_{c\,min}$ lacks a common meaning given the different theoretical approaches of the P–M and BT models, and so, the calibration of $r_{c\,min}$ is a model-specific problem. For the BT method, the value of $r_{c\,min}$ would need to be in the order of 40 s m^{-1}, compared to 50 s m^{-1} for the P–M method, for the estimated evaporation to approach the observed value of 51 mm for the period. A second potential problem is a limitation inherent to the Jarvis (1976) multiplicative approach for deriving the canopy resistance term. Owing to the linear nature of the algorithm there is potential for runaway increases in canopy resistance depending on the sensitivity of the equations used to derive the factors. This is of potential importance since plants typically increase their stomatal activity when it is needed most (i.e. during blooming), and likely in spite of the general atmospheric conditions if available water and energy are not limiting factors.

The use of a single reference value for $r_{c\,min}$, regardless of whether it is adjusted as a function of leaf area, assumes that optimal water use conditions apply for all plant phenological stages when water is not limiting. This precludes the potential for declining water use by plants when water availability is no longer crucial for maintaining overall plant health. For example, immediately following the peak evaporation period changes in leaf area become small but the plant may simply use less water. Adjusting the relative activity of plant stomata based on the timing of important life-cycle events (i.e. blooming) would require the incorporation of a detailed plant growth model. Examining changes in plant phenology or the timing of plant life-cycle events has been widely identified as a potentially important focus for climate change research (Beaubien and Johnson, 1994; Myneni *et al*., 1997; Schwartz, 1999; Spano *et al*., 1999; Chen *et al*., 2000; Wolfe *et al*., 2005). Ultimately, the consideration of a plant growth model would be a more physically based approach to modelling vegetation canopies, but would also vastly increase the complexity of point-scale evaporation modelling and provide considerable difficulties in dealing with complex landscapes comprised of several major plant species.

Daily evaporation estimates

Figure 6 compares modelled and observed evaporation over the course of daily optimal periods only. Modelled values represent the cumulative total over the entire day with negligible contributions for periods having a negative net supply of energy. The one-to-one line, r^2 values, and RMSE are also indicated in each graph. The first thing to note is that the r^2 values ($<0{\cdot}7$) are considerably reduced for the daily estimates compared to

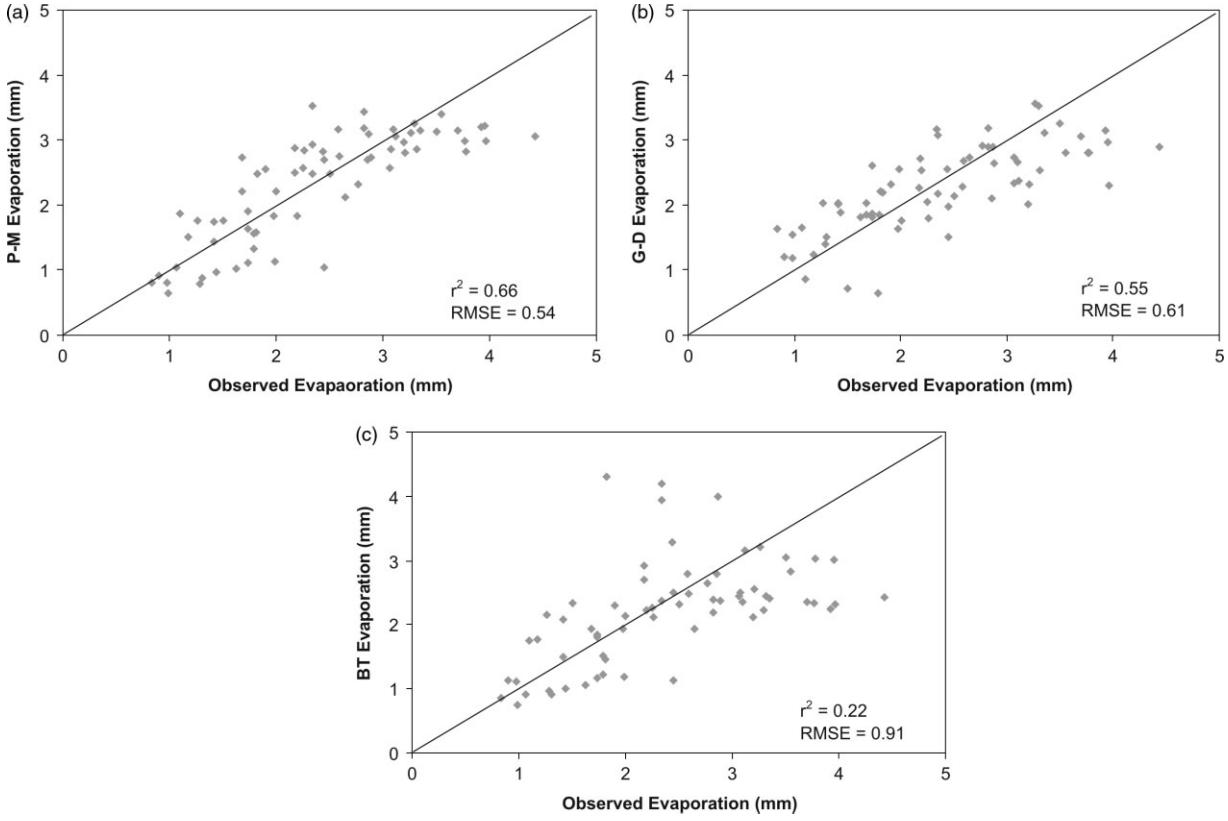

Figure 6. Optimal data period daily evaporation (mm), (a) P–M versus observed, (b) G–D versus observed, (c) BT versus observed. The one-to-one line is the diagonal line

DOI: 10.1002/hyp

those for the multi-day optimal periods. This is partly due to the increased number of data points considered versus only 10 for the multi-day comparisons. For the daily periods, each model tends to provide a similar number of evaporation estimates above and below the one-to-one line.

Overall, the P–M method provided the best results for daily estimates with an RMSE of ±0·5 mm day^{-1} while the G–D method followed closely with an associated error of ±0·6 mm day^{-1}. The BT method provided the poorest estimates overall with a low r^2 value (0·22) and an RMSE of almost ±1 mm day^{-1}. The BT method also showed the largest overestimations of evaporation which generally occurred during the period of 19–23 May, resulting in a modelled estimate that was nearly twice the observed value for the entire period (Table III). In this case, a lack of consideration for an effective canopy resistance (as a function of leaf area) is a possible factor in the large overestimate. This is because a 'full' canopy is assumed, and also because surface temperatures were relatively higher than those observed over most of the blooming period. Only an increase in the effective canopy resistance would offset the relatively higher surface temperatures (and increased saturated specific humidity) during this period since all other parameters were obtained by measurements.

Fifteen-minute-interval evaporation estimates

In Figure 7, modelled and observed evaporation for the 15-min average measurement periods are compared. The one-to-one line, r^2 values and RMSE are indicated in each graph. As was the case in the previous comparison, the statistics suggest the P–M method performed the best among the three methods. This is indicated by the slightly higher r^2 (0·77) and smaller RMSE (±0·014 mm/15-min interval) and more uniform scatter around the one-to-one line than that of the G–D method. The higher r^2 values between the modelled and measured evaporation for the 15-min intervals compared to the longer periods is again a result of the increased number of data points that now fall on the one-to-one line.

The scatter of the data points around the one-to-one line for all three methods appears to be similar to that for the daily periods shown in Figure 6. Given the large degree of scatter of the modelled vs. measured evaporation around the one-to-one line, it is unlikely that corrections for stability alone would rectify the relatively poor performance of the models but may potentially provide some improvement to the estimates.

COMPARISON OF MEASURED MAXIMUM DAILY EVAPORATION WITH PREVIOUS GRASSLAND STUDIES

Several previous studies have reported measured maximum daily rates of evaporation for various grassland regions (Verma *et al*., 1992; Kelliher *et al*., 1993; Meyers, 2001; Baldocchi *et al*., 2004; Burba and Verma, 2005; and Wever *et al*., 2002). This includes grassland sites located in both Canada (Saskatchewan, Alberta)

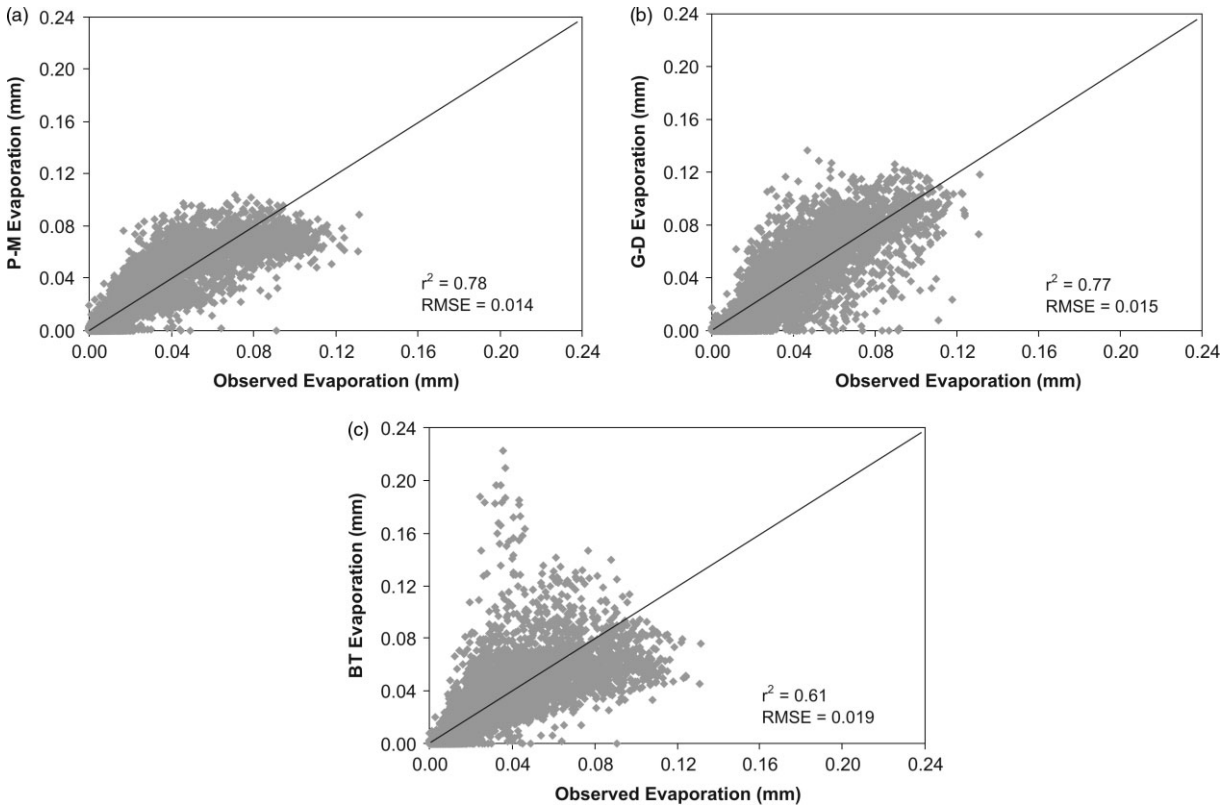

Figure 7. Fifteen-minute-interval evaporation (mm), (a) P–M versus observed, (b) G–D versus observed, (c) BT versus observed. The one-to-one line is the diagonal line

DOI: 10.1002/hyp

and the USA (Kansas, Oklahoma, and California). These studies have also used the eddy covariance method to obtained measurements of evaporative fluxes. Within the central Canadian prairie region, cool-season C_3 grasses tend to be the dominant plant species, while warm-season C_4 grasses dominate the central Great Plains region of the USA. Merely from a seasonal standpoint, a general difference between the two species is that cool-season C_3 grasses tend to reach their peak activity in the late spring to early summer period, whereas the warm-season C_4 grasses reach their peak activity towards mid to late summer. The measured maximum daily evaporation rate for the mixed-grass site at St Denis is approximately 4·4 mm day^{-1}. This is comparable to the measured maximum daily rates reported for the previous studies referred to below (Table IV).

It is interesting to note the relative consistencies reported for the maximum daily rates of evaporation for the various grassland regions, with the exception of the Kansas site. Some of the sites are characterized as tall grass sites (>1-m tall) while others are short grass sites (<0·50-m tall). Yet, the measured daily rates of evaporation for non-drought conditions are generally in the order of 4·5 mm on average regardless of the region studied and potential differences in biomass or leaf area. This is noteworthy since there are differences in the general climatic conditions of the regions, which have led to divergence in plant species. This suggests that the peak evaporation rate for prairie grasses in general under well-watered conditions would be close to 4·5 mm day^{-1}.

CONCLUSIONS

Three approaches to estimating 'actual' evaporation have been evaluated against eddy covariance measurements obtained at a mix-grassed upland site in the prairie region of central Saskatchewan. Comparisons with the observed data were limited to optimal periods when there was high confidence in the eddy covariance measurements. The three approaches include the P–M method which considers the control of plant stomata on transpiration, the G–D complimentary method that considers the relative evaporation as function of the humidity deficit and available energy, and a Dalton-type BT approach which directly considers the humidity gradient between the surface and atmosphere driven by surface temperature observations. For the P–M and the BT approaches, a common reference value of 62 s m^{-1} for the minimum surface resistance was specified. A Jarvis (1976) multiplicative scheme was used to parameterize the canopy resistance under the effects of environmental stresses using derived formulations suggested by Verseghy *et al*. (1993).

Based on a comparative analysis of r^2 and RMSE values for several time periods including 69 days of observations, daily, and 15-min intervals, the P–M method compared most closely to the observed values. For the multi-day optimal periods, the G–D method provided the best results for four periods compared to two for both the P–M and BT methods. Overall, the BT method provided the poorest agreement between modelled and measured evaporation. A possible reason for this could be the use of point measurements of surface temperature and soil moisture as a representative value for the variable flux footprint contributing to the measured flux at the sensors.

This may also be a result of the potential difficulties in applying a surface-temperature-driven BT model to a plant canopy. In 1802, Dalton showed that the rate of evaporation for a water surface depends on the difference between the saturated humidity at the surface temperature of the water and the dew point temperature of the overlying air. For the case of vegetation, adequately applying the flux gradient as a function of the surface temperature appears to be a more difficult problem. For example, early in the season, the BT method provided a large overestimate possibly due to the increased surface temperature and a lack of consideration for the relative number of stomata acting in parallel as a function of leaf area. However, there was considerably less effect on the P–M estimate, likely as a result of the combination approach.

In contrast, the BT model provided a considerable underestimate during the blooming period when the peak evaporation occurred and the leaf area was not likely a factor. Specifying a lower reference value of 50 s m^{-1} (compared to the original fitted value of 62 s m^{-1}) resulted in a much better estimate for the P–M method

Table IV. Maximum daily evaporation rates (mm d^{-1}) for several previous grassland studies

Source	Region	Dominant vegetation type	Water availability during growing period	Maximum evaporation rate (mm d^{-1}[a])
Verma *et al*. (1992)	Kansas (USA)	Warm-season C_4 grasses	Ample to dry	6·6
Kelliher *et al*. (1993)[a]	31–55° Latitude	Various grass species	Ample	4·8
Meyers (2001)	Oklahoma (USA)	Warm-season C_4 grasses	Ample	4·0
			Drought	2·5
Wever *et al*. (2002)	Alberta (Can)	Cool-season C_3 grasses	Ample	4·5
			Drought	3·0
Baldocchi *et al*. (2004)	California (USA)	Annual grass	Ample to dry	4·0
Burba and Verma (2005)	Oklahoma (USA)	Warm-season C_4 grasses	Ample	5·0

[a] Review paper which examined grassland regions for both southern and northern hemispheres. Maximum evaporation rate is the average value for the six studies examined.

DOI: 10.1002/hyp

but was less successful in the case of the BT method. This would indicate that the minimum reference value is highly model specific such that a common meaning may be virtually impossible to reconcile due to the theoretical differences in the model approaches. Further, the minimum reference value should be representative of the period for which plant activity generally peaks (i.e. during blooming). However, this value may not necessarily be applicable for the period immediately following peak evaporation when large declines in evaporation may be observed in lieu of any appreciable changes in atmospheric or soil moisture conditions.

Depending on the time scale of interest, modelled estimates of evaporation varied greatly between the methods. For instance, RMSE between modelled estimates and observations tended to be relatively high for daily periods ($>\pm 0{\cdot}5$ mm). For each model, the overall scatter around the one-to-one line for the daily and 15-min-interval periods remained similar. Model results for several multi-day periods, which ranged in length from 2 days to 2 weeks, showed reasonable agreement compared to observed values–this was reflected in the total evaporation for the 69 days of observations. As such, this study has demonstrated the general applicability of the models for estimating evaporation in a prairie landscape for multi-day time periods. But as the frequency of the estimates increased to daily and 15-min intervals, it was found that all three models provided less reliable estimates.

It is important to note that estimating evaporation over longer time periods (several days to weeks) may be appropriate for the purpose of long-term water balance calculations. However, estimates of water vapour fluxes (also heat and momentum) at the surface are needed for much shorter time scales for modelling atmospheric processes. Estimates for shorter time periods are also needed for calculating antecedent soil water content conditions for runoff calculations in hydrological models. This has important implications for flood monitoring and management. As such, relatively larger errors for daily and sub-daily periods may be unacceptable for many uses, such as for numerical weather prediction models and hydrological runoff models.

Improved resistance formulations need to be considered for more reliably estimating evaporation. The importance of plant controls on the transfer of water vapour to the atmosphere warrants continued research. Improved resistance formulations may want to consider the potential problem of using a single minimum reference value for canopy resistance. This value may be different for the blooming period, normally the period of peak evaporation, compared to that following the peak evaporation period due to reduced stomatal activity when differences in leaf area are likely negligible, and soil moisture and available energy are not limiting factors as opposed to a reduction in the number of stomata.

As suggested by the results in general, the G–D method which can be applied independently of land use (with the exception of water surfaces) provides a useful alternative to estimating a complex canopy resistance term. The G–D model performed surprisingly well for several periods of 2–3 days in duration but tended to perform more poorly for longer time periods. In the case of the BT method, there are apparent difficulties in using a simple parameterization to obtain reliable estimates of actual evaporation at the land surface. The canopy resistance term has a considerable influence on the rate of evaporation for the aerodynamic approach. Reconciling the relationship between changes in surface temperature and the surface resistance for plant canopies would also appear to be a difficult task.

Still, a Dalton-type BT approach remains attractive since it has practical application for both land and water surfaces, and has the potential for directly integrating observations of surface temperature. This has potential implications for studies concerning climate change or even characterizing severe drought, which is typical of prairie environments. Increased surface temperatures are likely to occur under conditions of reduced water availability, resulting in feedbacks to the atmosphere. Improvements to the simple BT method used here should consider an improved resistance formulation that covers the complete range of plant-specific and phenological stages of growth.

The potential effects of spatially varying driving factors of evaporation also warrant consideration. For example, explicitly accounting for spatial variations in surface temperature, soil moisture, turbulent transfer, and vegetation characteristics over the variable flux footprint may provide more reliable model estimates. This may provide a better understanding of how small-scale variability at the land surface affects modelled estimates of evaporation. If this were to be the case, this would help to better understand the effects of spatial variability on larger-scale fluxes and improve evaporation estimates required for hydrological and atmospheric modelling purposes.

ACKNOWLEDGMENTS

Funding support for this study was provided by the Drought Research Initiative (Canadian Foundation for Climate and Atmospheric Sciences (CFCAS)) and the Canada Research Chairs programme. The authors would also like to thank the Canadian Wildlife Service (Environment Canada) for access to the St Denis National Wildlife Area. Special thanks to Michael Solohub (field technical support) and Tom Brown (modelling support) at the Centre for Hydrology, University of Saskatchewan, Saskatoon.

REFERENCES

Baldocchi DD, Xu L, Kiang NY. 2004. How plant functional-type, weather, seasonal drought, and soil physical properties alter water and energy fluxes of an oak-grass savanna and an annual grassland. *Agricultural and Forest Meteorology* **123**: 13–39.

Beaubien EG, Johnson DL. 1994. Flowering plant phenology and weather in Alberta, Canada. *International Journal of Biometeorology* **38**: 23–27.

DOI: 10.1002/hyp

Bouchet RJ. 1963. Evapotranspiration réelle et potentielle: Signification climatique. *General Assembly, Berkeley, International Association of Scientific Hydrology* **62**: 134–142.

Brutsaert W. 1982. *Evaporation into the Atmosphere*. D. Reidel: Hingham, MA; 299.

Burba GG, Verma SB. 2005. Seasonal and interannual variability in evapotranspiration of native tallgrass prairie and cultivated wheat ecosystems. *Agricultural and Forest Meteorology* **135**: 190–201.

Campbell GS. 1974. A simple method for determining unsaturated hydraulic conductivity from moisture retention data. *Soil Science* **117**: 311–314.

Chen X, Tan Z, Schwartz MD, Xu C. 2000. Determining the growing season of land vegetation on the basis of plant phenology and satellite data in Northern China. *International Journal of Biometeorology* **44**: 97–101.

Crago R, Crowley R. 2005. Complementary relationships for near-instantaneous evaporation. *Journal of Hydrology* **300**: 199–211.

Granger RJ. 1989. An examination of the concept of potential evaporation. *Journal of Hydrology* **111**: 9–19.

Granger RJ, Gray DM. 1989. Evaporation from natural nonsaturated surfaces. *Journal of Hydrology* **111**: 21–29.

Granger RJ, Pomeroy JW. 1997. Sustainability of the western Canadian boreal forest under changing hydrological conditions—2-summer energy and water use. In *Sustainability of Water Resources under Increasing Uncertainty*, Rosjberg D, Boutayeb N, Gustard A, Kundzewicz Z, Rasmussen P (eds). IAHS Publication No. 240,IAHS Press: Wallingford; 243–250.

Jarvis PG. 1976. The interpretation of the variations in leaf water potential and stomatal conductance found in canopies in the field. *Philosophical Transactions of the Royal Society of London Series B-Biological Sciences* **273**(927): 593–610, A Discussion on Water Relations of Plants.

Kelliher FM, Leuning R, Schulze ED. 1993. Evaporation and canopy characteristics of coniferous forests and grasslands—Review. *Oecologia* **95**: 153–163.

Lhomme JP, Guilioni L. 2006. Comments on some articles about the complementary relationship. *Journal of Hydrology* **323**: 1–3.

Mahrt L. 1996. The bulk aerodynamic formulation over heterogeneous surfaces. *Boundary-Layer Meteorology* **78**: 87–119.

Meyers TP. 2001. A comparison of summertime water and CO_2 fluxes over rangeland for well watered and drought conditions. *Agricultural and Forest Meteorology* **106**: 205–214.

Monteith JL. 1965. Evaporation and environment. *Symposia of the Society for Experimental Biology* **19**: 205–234.

Myneni RB, Keeling CD, Tucker CJ, Asrar G, Nemani RR. 1997. Increased plant growth in the northern high latitudes from 1981–1991. *Nature* **386**: 698–702.

Penman HL. 1947. Evaporation in nature. *Reports on Progress in Physics* **11**: 366–388.

Penman HL. 1948. Natural evaporation from open water, bare soil and grass. *Proceedings of the Royal Society of London Series A-Mathematical and Physical Sciences* **193**: 120–146.

Pomeroy JW, Granger RJ, Pietroniro A, Elliott JE, Toth B, Hedstrom N. 1997. Hydrological Pathways in the Prince Albert Model Forest, Final Report to the Prince Albert Model Forest Association. Environment Canada, NHRI Contribution Series No. CS-97004. 154, + appendices.

Pomeroy JW, Gray DM, Brown T, Hedstrom NR, Quinton WL, Granger RJ, Carey SK. 2007. The cold regions hydrological model, a platform for basing process representation and model structure on physical evidence. *Hydrological Processes* **21**: 2650–2667.

Raddatz RL, Cummine JD. 2003. Inter-annual variability of moisture flux from the Prairie agro-ecosystem: Impact of crop phenology on the seasonal pattern of tornado days. *Boundary-Layer Meteorology* **106**: 2283–2295.

Schwartz MD. 1999. Advancing to full bloom: planning phenological research for the 21st century. *International Journal of Biometeorology* **42**: 113–118.

Sellers PJ, Dickinson RE, Randall DA, Betts AK, Hall FG, Berry JA, Collatz GJ, Denning AS, Mooney HA, Nobre CA, Sato N, Field CB, Henderson-Sellers A. 1997. Modelling the exchanges of energy, water, and carbon between continents and the atmosphere. *Science* **275**: 502–509.

Shen Y, Kondoh A, Changyuan T, Yongqiang Z, Jianyao C, Weiqiang L, Sakura Y, Changming L, Tanaka T, Shimada J. 2002. Measurement and analysis of evapotranspiration and surface conductance of a wheat canopy. *Hydrological Processes* **16**: 2173–2187.

Shuttleworth WJ, Wallace JS. 1985. Evaporation from sparse crops—an energy combination theory. *Quarterly Journal of the Royal Meteorological Society* **111**: 839–855.

Spano D, Cesaraccio C, Duce P, Snyder R. 1999. Phenological stages of natural species and their use as climate indicators. *International Journal of Biometeorology* **42**: 124–133.

Stannard DI. 1993. Comparison of Penman-Monteith, Shuttleworth-Wallace, and modified Priestley-Taylor evaporation models for wildland vegetation in semiarid rangeland. *Water Resources Research* **29**: 1379–1392.

van der Kamp G, Hayashi M, Gallén D. 2003. Comparing the hydrology of grassed and cultivated catchments in the semi-arid Canadian prairies. *Hydrological Processes* **17**: 559–575.

Verma SB, Kim J, Clement RJ. 1992. Momentum, water vapor, and carbon dioxide exchange at a centrally located prairie site during FIFE. *Journal of Geophysical Research* **97**: 18629–18639.

Verseghy DL, McFarlane NA, Lazare M. 1993. A Canadian land surface scheme for GCMs : II. Vegetation model and coupled runs. *International Journal of Climatology* **13**: 347–370.

Wever LA, Flanagan LB, Carlson PJ. 2002. Seasonal and interannual variation in evapotranspiration, energy balance and surface conductance in a northern temperate grassland. *Agricultural and Forest Meteorology* **112**: 31–49.

Wilczak JM, Oncley SP, Stage SA. 2001. Sonic anemometer tilt correction algorithms. *Boundary-Layer Meteorology* **99**: 127–150.

Wolfe DW, Schwartz MD, Lakso AN, Otsuki Y, Pool RM, Shaulis NJ. 2005. Climate change and shifts in spring phenology of three horticultural woody perennials in northeastern USA. *International Journal of Biometeorology* **49**: 3003–3309.

Yates TT, Si BC, Farrell RE, Pennock DJ. 2006. Probability distribution and spatial dependence of nitrous oxide emission: temporal change in hummocky terrain. *Soil Science Society of America Journal* **70**: 753–762.

DOI: 10.1002/hyp